JOURNAL OF MATERIALS SCIENCE 26 (1991) 3869–3873

Mechanical stability of sol–gel films

A. ATKINSON, R. M. GUPPY
AEA Technology, Building 429, Harwell Laboratory, Didcot, Oxon. OX11 0RA, UK

The relationship between film cracking and film thickness has been studied experimentally for films of ceria gel deposited by spinning on to stainless steel substrates from an aqueous ceria sol. A critical film thickness below which films were crack-free was observed at about 0.6 μm. For films thicker than the critical thickness the crack spacing was approximately ten times the film thickness. Existing models for the mechanical stability of the films were examined to explain the observations, encompassing different forms of relaxation of the stress in the vicinity of a crack through the film. The model in best accord with the experimental observations is one in which stable delamination cracks are formed at the film–substrate interface on both sides of a crack through the film. However, for the model to be applicable some rather restrictive conditions must be assumed to be satisfied.

1. Introduction

Ceramic thin films have a wide range of applications in optics, electronics, catalysis and corrosion protection. The gel processing route (often referred to as sol–gel) is particularly attractive for fabricating ceramic films, since the liquid precursor can easily be applied to a substrate by spinning, dipping or spraying. The two principal gel-processing routes for oxide ceramics involve the gelation of either a particulate aqueous dispersion of hydrated oxides (sol) by removal of water, or the cross-linking of inorganic polymers by hydrolysis of metal alkoxides in an alcoholic solvent [1]. For both routes, final conversion to the oxide is accomplished by heat-treating the gel. Also, in both routes, there are large shrinkages to accommodate at two stages: as the gel dries, and as the dried gel sinters to dense ceramic. The shrinkage induces tensile stress in the film and the result is often cracking through the film and delamination at the interface. Thus it is difficult to produce ceramic films thicker than one micrometre in a single deposition by this process [2]. In this paper we report the results of experiments to investigate the nature of these mechanical instabilities as a function of film thickness for films of cerium oxide, prepared by the aqueous sol–gel route and applied by spinning to stainless steel substrates.

2. Experimental procedure

2.1. Preparation of films

Ceria sol was prepared by peptizing a slurry of cerium hydroxide (Rhône Poulenc, 98 grade), after washing in demineralized water, with nitric acid at a nitrate to ceria mole ratio of 0.27. This sol contained de-aggregated primary particles about 8 nm in size [3]. The sols were prepared with ceria concentrations ranging from 225 to 450 $g l^{-1}$. Stainless steel disc substrates of 27 mm diameter and 0.5 mm thickness were polished to a mirror finish with 1 μm diamond paste, ultrasonically cleaned in acetone and weighed. The substrates were coated using a spin-coater in a Class 100 clean room. The thickness of the coating was controlled by a combination of spin speed and sol viscosity and the films gelled while spinning (in less than one minute).

The coated substrates were examined by optical microscopy and reweighed to determine the mass of gel, from which the equivalent gel thickness was calculated. The density of gel was determined on larger free-standing gel pieces dried under the same conditions (1.22 to 1.40 $g ml^{-1}$, depending on ceria concentration). In estimating film thickness we assumed that the gel density was independent of film thickness. The coated substrates were heat-treated at 500 °C in air for 30 min and re-examined. Fifteen films were prepared with equivalent gel thicknesses in the range 0.34 to 2.07 μm.

2.2. Mechanical stability

The observations clearly demonstrated the existence of a critical film thickness (between 0.54 and 0.61 μm) below which the film was uniform, adherent and free of cracks. The 0.61 μm film showed the initiation of through-film cracking in the form of isolated crack segments (Fig. 1a). The cracks appear to have nucleated homogeneously and are not preferentially associated with scratches on the substrate. When the equivalent thickness reached 0.79 μm (Fig. 1b) the crack pattern was interconnected and became coarser as the film thickness increased further (Fig. 1c and d). The spacing between cracks as a function of equivalent film thickness was measured by taking mean linear intercepts from micrographs such as those in Fig. 1. A plot of crack spacing against gel thickness (Fig. 2) reveals a linear relationship between the two variables. The

0022–2461/91 $03.00 + .12

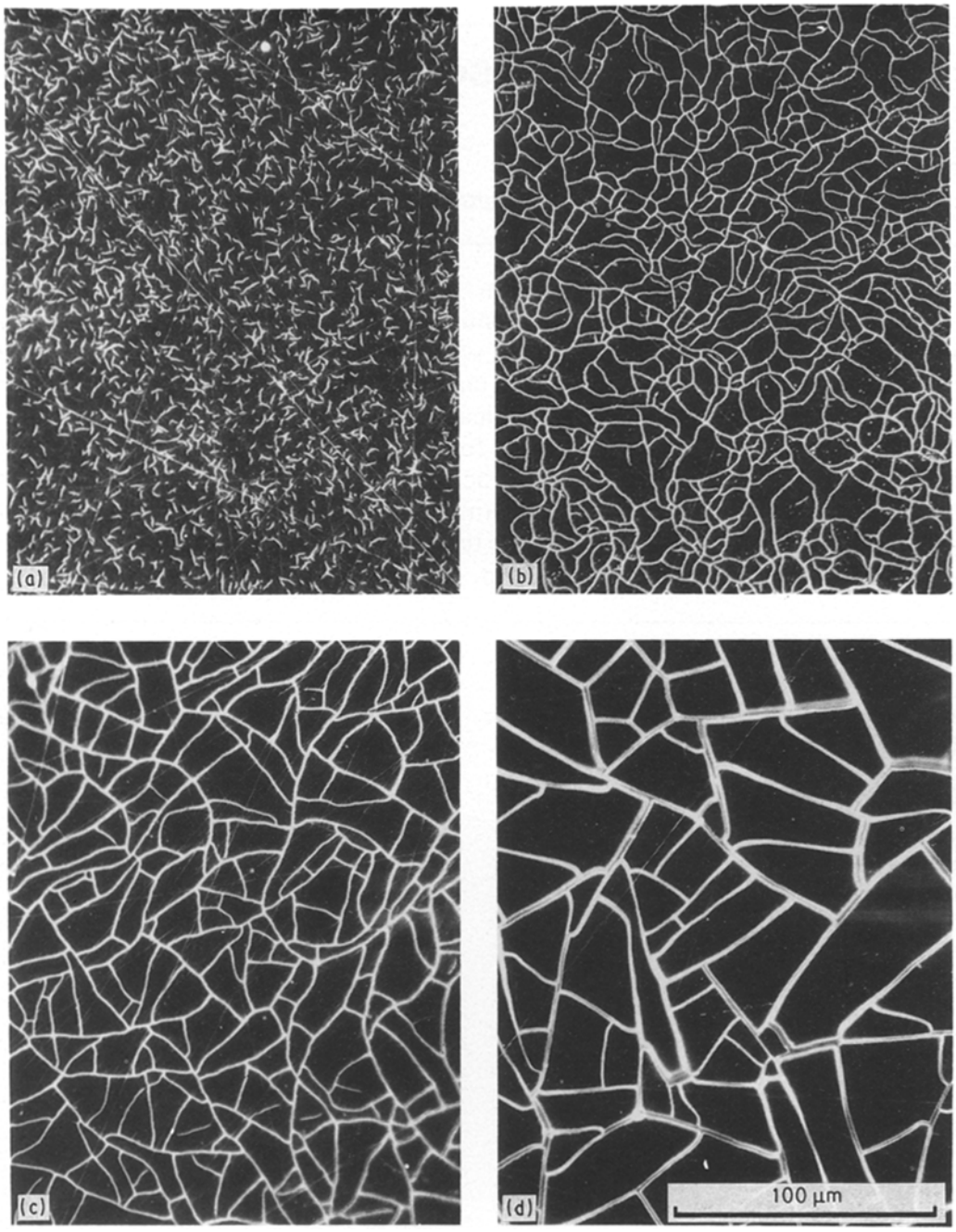

Figure 1 Optical micrographs of the crack patterns in ceria gel films of different thickness on stainless steel substrates: (a) 0.61 μm, (b) 0.79 μm, (c) 1.02 μm, (d) 2.07 μm.

failure of the thickest films clearly involved delamination at the interface as well as through-film cracking, since optical interference fringes from the film–substrate air gap could be seen. We cannot be certain, from direct observation, whether delamination also occurred in the thinner films (about 1 μm thickness), or not. Indirect evidence for delamination is provided in the discussion.

3. Discussion

3.1. Film cracking

The cracking and delamination of thin films is a subject having wide applicability, from the drying of paint to microelectronic materials. The formation of cracks through a brittle film in uniaxial tension on a substrate has been analysed by Hu *et al.* [4]. They concluded that, just as in a bulk material, a flaw of depth c (and of length greater than the film thickness) would become unstable and extend through the thickness of the film when

$$1.2\pi\sigma^2 c > EG_f \quad (1)$$

where σ is the stress in the film, E is the modulus of both the film and the substrate (assumed equal) and G_f is the critical strain energy release rate for crack extension in the film (equal to twice the surface energy for a brittle fracture). This expression is unable to account for a critical film thickness above which defects propagate as cracks unless it is postulated that the defect size is a function of film thickness, h.

Hu *et al.* [4] also considered the extension of a localized through-film crack across the substrate.

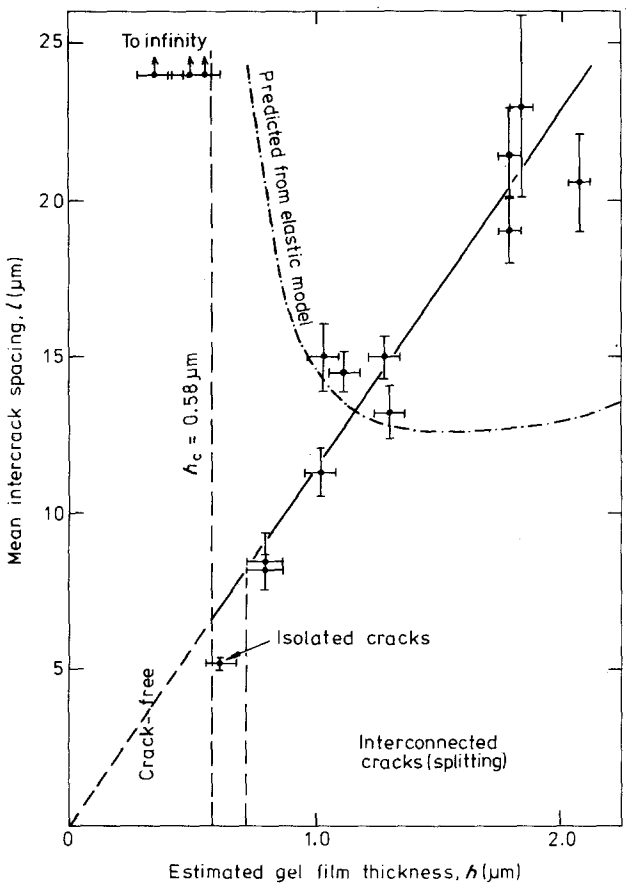

Figure 2 The relationship between mean crack spacing and thickness of the gel film. The error bars on the data points are standard errors on the mean and are not the standard deviation of the distribution of crack spacings. The dot-dash curve is the relationship predicted assuming only elastic relaxation around cracks through the film (see text).

They concluded that this would occur if

$$0.6\pi\sigma^2 h > EG_f \quad (2)$$

Equation 2 does predict the existence of a critical film thickness

$$h_c = \frac{EG_f}{0.6\pi\sigma^2} \quad (3)$$

Since the properties of the film and the stress in the uncracked parts of the film are expected to be independent of thickness, and determined by the state of dryness of the gel, Equation 3 could account for the observed critical thickness. However, the through-film crack must first be formed before it can be extended across the film and, from a comparison of Equations 1 and 2, this requires that the films contain flaws of depth greater than half the critical film thickness. (Throughout the discussion we assume, for simplicity, that the film and the substrate have the same modulus of elasticity, i.e. $E_f = E_s$. The numerical constants in Equations 1 to 3 are modified when $E_f \neq E_s$ [5]. In the present experiments we expect $E_f < E_s$ and, as a result, h_c will be increased relative to Equation 3 above.)

If the interface between film and substrate is sufficiently "weak" then interface delamination is expected to accompany film cracking. This situation was analysed by Hu and Evans [5] who concluded that if $G_f > 8G_i$ (where G_i is the effective fracture surface energy of the interface) film cracking and unstable delamination both occur; and if $G_f < 4G_i$ only film cracking occurs. In the intermediate range ($4G_i < G_f < 8G_i$) limited stable delamination is predicted, with a delaminated zone extending up to about five times the film thickness on both sides of the film crack. These different failure modes only influence h_c (in Equation 3) by changing the effective value of G. Since the values of the parameters are not known, the failure mode cannot be predicted, nor can it be deduced from the critical thickness.

3.2. Multiple cracking and crack spacing

3.2.1. Elastic relaxation

In a drying film the biaxial tensile stress in the plane of the film is monotonically increasing as the film continues to dry. The first long-range crack will occur when Equation 3 is satisfied, at the location of the largest pre-existing flaw (subject to the minimum requirement that it is equivalent to a localized crack extending more than half-way through the film thickness). The next long-range crack will form when the stress has increased sufficiently to activate the next largest flaw, and so on. If the distribution of such flaws is uniform on a scale that is small in comparison with the final inter-crack spacing, then the location of long-range cracks, subsequent to the first, will be determined by the maximum stress. The stress is not uniform, after the first crack, because the crack relaxes the stress in its vicinity. If this stress relaxation is elastic then the stress relaxation (Fig. 3) decays with distance, x, from the crack over a characteristic length approximately equal to the film thickness [6]:

$$\frac{\Delta\sigma}{\sigma} = -\frac{h}{x} \quad (4)$$

This approach predicts that new cracks will form midway between existing ones and was analysed by Grosskreutz and McNeil [7]. Following their approach, the crack spacing is given (for uniaxial stress) by

$$l \simeq \frac{4h}{\ln(\varepsilon_f/\varepsilon_c)} \quad (5)$$

where ε_c is the drying strain when the first crack occurs and ε_f is the final drying strain of a stress-free (free-standing) film. From Equation 3

$$\varepsilon_c = \left(\frac{G_f}{0.6\pi Eh}\right)^{1/2} \quad (6)$$

Furthermore, at the critical thickness h_c, $\varepsilon_c = \varepsilon_f$. Therefore Equation 5 can be rewritten as

$$l \simeq \frac{8h}{\ln(h/h_c)} \quad (7)$$

This function is plotted in Fig. 2 assuming h_c = 0.58 μm, the experimentally observed critical thickness. The elastic model of stress relaxation clearly is not in accordance with the experimental results. In particular, the elastic model predicts a crack spacing that decreases with film thickness in the range h_c to

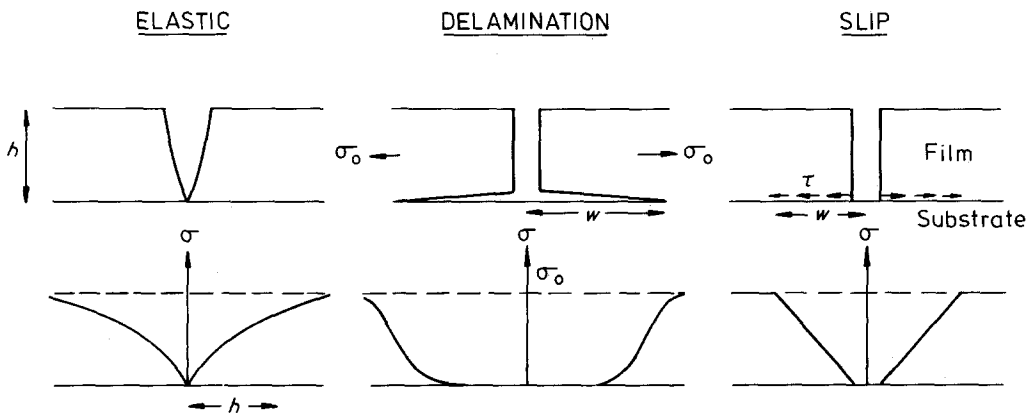

Figure 3 Schematic diagram illustrating the nature of the stress distribution in the vicinity of a crack, for different types of relaxation process.

$2h_c$. This is because, according to the model, the greater the strain to be relaxed by cracking, the closer are the cracks spaced. The critical cracking condition (Equation 6) predicts that thicker films first crack at lower strains (and lower stresses) than thinner ones. Since the average total strain is the same in all films (and equal to ε_f), the thicker films have a larger proportion of final strain associated with the greater crack density and a lower proportion associated with residual stress in the uncracked regions; hence the predicted fall in crack spacing with increasing film thickness.

Therefore we conclude that either the elastic model is inappropriate, or the crack spacing is controlled by the statistical distribution of flaws such that Equation 3 is not applicable.

3.2.2. Plastic relaxation

The failure of elastic relaxation to account for the observed relationship between crack spacing and film thickness implies that contributions from plastic deformation must be dominant. These could be

a) stable interfacial delamination,
b) unstable interfacial delamination,
c) shear at the film–substrate interface, and
d) visco-elastic relaxation of the film.

The effect of stable interfacial delamination would be to relax the stress in a region up to about the delamination width (w) on either side of the crack (Fig. 3). The effect of this may be estimated by noting that when the crack spacing is l the total strain in the film is

$$\varepsilon = \varepsilon_c + \frac{2w}{l}(\varepsilon_f - \varepsilon_c) \quad (8)$$

In the final state $\varepsilon = \varepsilon_f$ and therefore $l \simeq 2w$. The analysis of Hu and Evans [5] predicts that, at the cracking condition, w is proportional to h. The constant of proportionality may be up to about 5, depending on the ratio G_i/G_f. Thus, stable interfacial delamination would predict that $l \simeq 10\,h$ and this is consistent with the experimental observations, provided that the rather restrictive conditions on G_i/G_f are fulfilled ($1/8 < G_i/G_f < 1/4$). Hu and Evans observed this behaviour for Cr films on stressed stainless steel substrates.

If $G_i/G_f < 1/8$ then Hu and Evans [5] predict unstable interfacial delamination, and they observed this behaviour when the interface between Cr and stainless steel was contaminated. In this case, in principle, the whole film would delaminate from a single through-film crack. Whether this happens in practice will depend on a balance between the macroscopic strain rate (drying rate), which increases the probability of forming a new film crack, and the velocity at which the delamination propagates. Thus, predicting the crack spacing in this case is a time-dependent problem and is beyond the scope of this discussion.

Hu and Evans [5] also discuss stress relief by shear of the interface in the neighbourhood of the through-film cracks (Fig. 3). They assume that the interfacial shear relaxes the tensile stress in the film linearly over a characteristic width, w, given by

$$w = \sigma h/\tau \quad (9)$$

where τ is the shear strength of the interface. They concluded that this behaviour occurred for Cr films on Al substrates. σ is the stress in the film at cracking and, from Equation 3, $\sigma_c \propto h^{-1/2}$ so that $w \propto h^{1/2}$. The final crack spacing is predicted to be between w and 2w [7] and so we expect the crack spacing to be proportional to the square root of film thickness. The present experimental results are not consistent with this relationship.

The effect of stress relief by visco-elastic deformation has been analysed by Riedel [8] for oxide films on deforming metal substrates. (The situation is similar for films sintering on constraining substrates [9, 10].) Riedel concluded that the visco-elastic analysis could account for experimental observations on iron oxide scales grown thermally on low-alloy steel. The approach differs from those considered previously in that the strain rate (drying rate, in the system considered here) becomes an important variable. In particular, the critical thickness and crack spacing are expected to increase with decreasing strain rate. Riedel [8] included visco-elastic deformation of both the film (creep) and sliding of the interface. At high strain rates, interface sliding dominates and the crack spacing is given by

$$l = \left(\frac{8h\sigma_c}{\eta\dot{\varepsilon}}\right)^{1/2} \quad (10)$$

where η is a viscosity coefficient for the interface. Since σ_c is proportional to $h^{-1/2}$, Equation 10 predicts that the crack spacing is proportional to $h^{1/4}$ for constant strain rate. Whether the strain rate for the drying films is constant, or not, is unknown. We may speculate that the thicker films would dry more slowly than thinner films by out-diffusion of water vapour through the film. In such a case the strain rate will not be constant and will also decrease as h increases; i.e. $\dot{\varepsilon} \propto h^{-n}$, where n is unity for a steady-state loss of water. If this is the case the crack spacing will be proportional to $h^{3/4}$. Thus viscous sliding of the interface could explain the results of the present experiments.

In summary, the model of Hu and Evans [5] for interfacial shear does not account for the experimental results because it predicts a crack spacing proportional to the square root of film thickness, whereas a linear relationship is observed. It is possible to come close to a linear relationship if interfacial viscous sliding (time-dependent) occurs provided that the strain rate decreases with increasing film thickness. However, the model most consistent with the experimental observations is one in which limited interfacial delamination accompanies film cracking. This model correctly predicts the observed linear relationship and the approximate magnitude of the constant of proportionality.

4. Conclusions

The experiments reveal that gel films of ceria deposited on stainless steel substrates from aqueous colloidal sols become mechanically unstable to cracking at a critical thickness of about 0.6 μm. The existence of a critical thickness is consistent with the predictions of the model of Hu *et al.* [4] in which the key event is the lateral growth across the film surface of a short-range crack through the film. For films thicker than the critical thickness, the spacing between cracks is observed to be approximately equal to ten times the film thickness. This can be explained by the model of Hu and Evans [5] in which limited delamination at the film–substrate interface accompanies film cracking. The conditions necessary for these models to be applicable are, nevertheless, rather restrictive. First, there must be a population of pre-existing defects of size greater than half the film thickness. Second, the ratio of interfacial fracture energy, G_i, to the film fracture energy, G_f, must fall in the range 0.125 to 0.25.

The models considered here were all developed for a system with uniaxial and uniform applied stress. The resulting crack geometry in such a case is a series of cracks perpendicular to the direction of stress. In the present films the stress is biaxial, leading to a two-dimensional crack pattern. This crack geometry has been reproduced in both computer models [11] and experimental models [12] and is known to have fractal nature. Furthermore, the stresses in drying gel films are expected to vary with depth in the film [13]. Therefore, the models discussed in this paper should be regarded as only an indicative approximation to the real situation.

5. Acknowledgement

We are grateful to D. L. Segal for provision of the ceria sol. This work forms part of the programme of corporate research carried out by the UK Atomic Energy Authority.

References

1. D. L. SEGAL, "Chemical Synthesis of Advanced Ceramic Materials" (Cambridge University Press, Cambridge, 1989).
2. L. C. KLEIN (ed.), "Sol-Gel Technology for Thin Films, Fibers, Preforms, Electronics and Specialty Shapes" (Noyes, New Jersey, 1988).
3. J. L. WOODHEAD, UK Patent 1 342 893 (1974).
4. M. S. HU, M. D. THOULESS and A. G. EVANS, *Acta Metall.* **36** (1988) 1301.
5. M. S. HU and A. G. EVANS, *ibid.* **37** (1989) 917.
6. M. MURAKAMI, CRC Crit. *Rev. Solid State Mater. Sci.* **11** (1984) 317.
7. J. C. GROSSKREUTZ and M. B. McNEIL, *J. Appl. Phys.* **40** (1969) 355.
8. H. RIEDEL, *Metal Sci.* **16** (1982) 569.
9. G. W. SCHERER and T. GARINO, *J. Amer. Ceram. Soc.* **68** (1985) 216.
10. R. K. BORDIA and R. RAJ, *ibid.* **68** (1985) 287.
11. P. MEAKIN, *Thin Solid Films* **151** (1987) 165.
12. A. J. SKJELTORP and P. MEAKIN, *Nature* **335** (1988) 424.
13. G. W. SCHERER, *J. Non-Cryst. Solids* **89** (1987) 217.

Received 11 April
and accepted 19 November 1990